Adhesion, spreading, and proliferation of endothelial cells on charged hydrogels

Yong Mei Chen [a,b], Jing Jing Yang [b], Jian Ping Gong[b,] *

[a]*Department of Chemistry, School of Science, Xi'an Jiaotong University, Xi'an 710049, CHINA*

[b]*Graduate School of Science, Hokkaido University, Sapporo 060-0810, JAPAN*

*Corresponding authors: J. P. Gong, gong@sci.hokudai.ac.jp, Tel & Fax: 81-11-706-2774

Abstract

As soft and wet scaffolds, hydrogels are attractive materials for tissue engineering due to their similarity in structure and properties to living tissue. For designing hydrogels as potential artificial tissues, some basic requirements, such as a high level of cellular viability, suitable viscoelasticity, and high mechanical strength are required. However, it is difficult to develop a hydrogel that satisfies even two of these requirements at the same time. In this review, our recent advances in developing synthetic hydrogels as cell culture scaffold are summarized. We found that endothelial cells (ECs) can proliferate directly on some synthetic hydrogels with negatively charge, so long as the hydrogels have a Zeta potential lower than *c.a.* -20 mV , and the cell behavior can be controlled by adjusting the hydrogel's charge density. Furthermore, confluent EC monolayers cultured on the hydrogels show excellent platelet compatibility, compared to EC monolayer cultured on polystyrene plate. On the basis of the above study, we have further developed micro-patterned hydrogels for selective cell spreading, proliferation, and orientation. We have also developed tough hydrogels on which cells show viability. These results will promote the potential applications of synthetic hydrogels in tissue engineering.

Key words: Hydrogel; Endothelial cell; Cell culture scaffold; Platelet adhesion; Microfabrication; Tissue engineering

1. Introduction

Hydrogel consists of cross-linked hydrophilic polymer networks swollen with large amounts of water [1]. Normally, the water content is more than 50 % of the total weight when we use the term “hydrogel”. Hydrogels are solids on the macroscopic scale: they have definite shapes and do not flow, deform with stress and recover their initial shape after removing of stress. At the same time, they behave like solutions on the molecular scale: water-soluble molecules can diffuse in hydrogels with various diffusion constants reflecting the sizes and shapes of the molecules. Therefore, hydrogels are becoming especially attractive in the application as scaffolds for repairing and regenerating a wide variety of tissues and organs, or even as substitutes of tissues and organs since their three-dimensional network structure and viscoelasticity are similar to the macromolecular-based extracellular matrix (ECM) in biological tissue [2].

In designing hydrogels potentially useful as artificial tissues, cellular viability, high mechanical strength, and biocompatibility are required. However, to be qualified for biological applications, significant problems and shortfalls of hydrogels should be solved, including: 1) Improving the cytocompatibility of hydrogel. The role of tissue cells is important in biological activity. For example, a continuous endothelial cell (EC) monolayer in the inner surface of a blood vessel contributes to protecting procoagulant activity [3, 4]. Another example is cartilage cells synthesizing the ECM that contributes to load-bearing and lubrication of cartilage [5, 6]. However, most hydrogels do not promote cellular viability, excepting collagen and fibrin hydrogels obtained from natural macromolecules. 2) Improving the mechanical strength of hydrogel. In the physiological condition, many tissues, such as blood vessels, articular cartilages, semi-lunar cartilages, tendons, and ligaments exist in a severe mechanical dynamic environment. For example, articular cartilage sustains a daily compression of 3~18 MPa, while most hydrogels only can sustain a few kPa compression.

These shortages greatly prevent the wide application of hydrogels in tissue engineering field. Thus, from a potentially practical view point, in order to replace the natural tissues with hydrogels, design and production of hydrogels with some critical parameters, such as high mechanical strength and cellular viability, are crucially important in the biomedical applications of hydrogels. Polymer scientists have strived to design hydrogels with these critical parameters by using synthetic polymers in addition to natural polymers, because synthetic hydrogels have many advantages over natural source like collagen: The chemical properties of synthetic hydrogels are easily controllable, reproducible, they are infection-free, withstand high-temperature sterilization, and relatively low cost.

In this review, our recent progress on the study of cells adhesion and proliferation on protein-free synthetic polymer hydrogels, platelet adhesion on the EC monolayers cultured on hydrogels, as well as some examples of application of hydrogels in tissue engineering, such as designing micro-patterned hydrogels for cell orientation, tough hydrogels for cell adhesion and proliferation, will be introduced. Studying cell behavior on synthetic hydrogels with defined chemical structure and tunable materials properties is helpful for understanding the conditions that control cell behavior, and may be broadly applicable to design and select proper polymer materials in tissue engineering applications.

2. Experimental

Materials

2-Acrylamido-2-methyl-propane sulfonic acid sodium salt (NaAMPS), as a monomer, was obtained by neutralization of 2-acrylamido-2-methyl-propane sulfonic acid (Tokyo Kasei Kogyo, Tokyo, Japan) with sodium hydroxide in ethanol, and purified by recrystallization from acetone. Sodium *p*-styrene sulfonate (NaSS; Tokyo Kasei Kogyo, Tokyo, Japan), as a monomer, was purified by recrystallization from ethanol, dried at 25 °C in vacuo. Acrylic acid (AA; Kanto Chemicals, Tokyo, Japan), as a monomer, and methacrylic acid (MAA;

Kanto Chemicals, Tokyo, Japan), as a monomer, were distilled at a reduced pressure. Acrylamide (AAm; Junsei chemicals, Tokyo, Japan), as a monomer, was purified by recrystallization from chloroform. *N, N*-dimethylacrylamide (DMAAm; Tokyo Kasei Kogyo, Tokyo, Japan), as a monomer, was distilled at a reduced pressure. *N, N′*-methylenebis-(acrylamide) (MBAA; Tokyo Kasei Kogyo, Tokyo, Japan), as a cross-linking agent, was purified by recrystallization from ethanol. Poly (vinyl alcohol) (PVA; Mw = 95000, Wako Pure Chemicals, Osaka, Japan), as a polymer, glutaraldehyde (50% aqueous solution, Kanto Chemicals, Tokyo, Japan), as a cross-linking agent, and 2-oxoglutaric acid (Wako Pure Chemicals, Osaka, Japan) as an initiator, were used as purchased.

Hydrogel synthesis

Sheet-shaped homopolymer hydrogels, poly(2-acrylamido-2-methyl-propane sulfonic acid sodium salt) (PNaAMPS), poly(sodium *p*-styrene sulfonate) (PNaSS), poly(acrylic acid) (PAA), poly(methacrylic acid) (PMAA), polyacrylamide (PAAm), and poly(*N, N* –dimethylacrylamide) (PDMAAm), as well as copolymer hydrogels, poly(NaAMPS-*co*-DMAAm) with various molar fractions (F) of NaAMPS, were synthesized by radical polymerization. An aqueous solution of 1 M monomer, 1-10 mol% cross-linker (MBAA) in respect to the monomer concentration, and 0.1 mol% initiator (2-oxoglutaric acid), were introduced into the reaction cells. After being purged with nitrogen gas for 30 min, the reaction cells was irradiated with UV light (wavelength, 365 nm) to facilitate polymerization at room temperature for 6 h.

Poly(vinyl alcohol) (PVA) gel was prepared by reacting with the cross-linker, glutaraldehyde. Aqueous solution contained 5 wt% PVA, 1, 2, 4, 6, and 10 mol% cross-linker in respect to the monomer concentration was prepared first, and 0.2 N HCl was dropped into the PVA aqueous solution to adjust the pH of the reaction solution to 2. Then the PVA solution was introduced into the reaction cells for gelation at room temperature for 24 h.

All the gel reaction was carried out in the reaction cells that were formed by two parallel glass

plates separated by a silicone spacer of 1-mm thickness. After gelation, the gels were removed from the glass cells and immersed in a large volume of ion-exchanged water for 1 week. During this period, the water was changed 2 times every day in order to remove residual chemicals. The pH and ionic strength of the solution contained in the gels were then adjusted to 7.4 and *ca.* 0.15 M, respectively, by immersing the gels in HEPES (Sigma-Aldrich Co., Saint Louis, USA) buffer solution (HEPES, 5×10^{-3} M; $NaHCO_3$, 1.55×10^{-2} M; NaCl, 0.14 M; pH, 7.4). The degree of swelling of a gel (q) is measured as the weight ratio of the gel in its equilibrated state HEPES buffer solution to that in its dried state. Each value was averaged over at least three parallel measurements.

Zeta potential (ζ) measurement

The Zeta potential (ζ) of hydrogels was determined by using gel particles. Bulk gel was stirred in 50 mL HEPES buffer solution in order to generate particles of radius *ca.* 1 μm. The electrophoretic mobility of gel particles dispersed in HEPES buffer solution was measured by Rank mark II microelectrophoresis apparatus (Rank Brothers, Cambridge, England), and ζ was calculated using the Smoluchowski equation. For statistical purposes, values from at least 70 reading points were recorded for each gel. The Zeta potential, ξ(V), was calculated using Smoluchowski equation as follows:

$$u = \frac{v}{E} = \frac{\varepsilon\xi}{\eta}$$

Here u is the electrophoretic mobility of a particle$(m^2/(V \cdot s))$, v is the velocity of the particle(m/s), which was calculated by a computer analysis program "MetaMorph" (Nippon ROPER Co., Chiba, Japan), E is applied electric field (V/*m*), ε is the dielectric constant of liquid, and η is the viscosity of liquid. Using $\varepsilon = 6.937 \times 10^{-10} C^2 J^{-1} m^{-1}$ and $\eta = 8.903 \times 10^{-4} Pa \cdot s$ for water at 25°C, $E = V/d$, where V = 49V is the applied voltage, and $d = 5.16 \times 10^{-2} m$ cm is the distance between the electrodes, we have, $\xi = 1.35 \times 10^3 v$.

Protein adsorption

The amount of protein contained in cell culture medium that adsorbed on the surface of the poly(NaAMPS-*co*-DMAAm) gels was quantitatively characterized by recovering the protein adsorbed on the surface of the gels. The poly(NaAMPS-*co*-DMAAm) gel disks with a diameter of 2.5 cm were exposed to 1.67 ml of 20% (v/v) fetal bovine serum (FBS) containing cell culture medium for 6 h at 37°C in a humidified atmosphere of 5% CO_2. Then the gels were taken out from the medium and were gently rinsed by ice-cold phosphate-buffered saline (PBS) buffer (pH = 7.4). The adsorbed proteins were desorbed with 100-μl ice-cold lysis buffer (0.05M Tris–HCl, 0.15M NaCl, 0.001M EDTA, and 0.5% Triton X-100), with freshly added 1% (v/v) protease inhibitor cocktail (protease inhibitor cocktail set III, Calbiochem, La Jolla, CA) over ice. The lysate was collected in a microfuge tube. The proteins content in the lysates were measured by spectrophotometer at 595 nm.

The amount of fibronectin adsorbed on the surface of the gels was quantitatively characterized via immuno-fluorescence. The poly(NaAMPS-*co*-DMAAm) gels with a diameter of 1.5 mm were exposed to 1 ml of 20% (v/v) FBS in PBS solution for 6 h at 37°C in a humidified atmosphere of 5% CO_2. The same gels blocked with 1% (w/w) bovine serum albumin (BSA) (Sigma) in PBS solution were used as controls. After washing with 1 ml PBS for three times, gels were incubated with 1 ml 1:200 dilution of FITC-conjugated antifibronectin (Biogenesis Ltd., UK) for 2 h at 37°C in a humidified atmosphere of 5% CO_2 and then washed for three times with 1 ml PBS. The immunostained samples were analyzed by a fluorescence confocal laser scanning microscope (OLYMPUS, Co., Tokyo, Japan) equipped with a 20× objective. The fluorescence intensity difference between the gels incubated in FBS and BSA, corresponding to the amount of absorbed fibronectin on gel surfaces, was measured.

Cell culture

After sterilization by autoclaving (120˚C, 20 min), the gels disks (diameter is 15 mm and thickness is *ca.* 2 mm) equilibrated in HEPES buffer solution were used for BFAEC and

HUVEC culture. Then the gel disk was placed in a 24-well polystyrene tissue culture dish. A BFAEC or HUVEC suspension (2.26×10^4 cells/cm^2 in 20% FBS Medium-199) was directly seeded on the gel surfaces that not been modified by any cell-adhesive proteins or peptides before cell culture. The cell-loaded samples were cultured at 37°C in a humidified atmosphere of 5% CO_2. Cell morphology and proliferation on the gel surface was monitored using an OLYMPUS IX 71 phase contrast microscope (OLYMPUS Co., Tokyo, Japan) equipped with a digital camera using 10× objectives.

3. Adhesion and proliferation of cells on protein-free synthetic polymer hydrogels

To mimic the macromolecular-based ECM in living tissue, facilitating cell adhesion and proliferation is a basic requirement for hydrogels. However, various hydrogels that are derived from natural resources, such as alginate, and chitosan, as well as those that are synthetically created, such as poly(ethylene oxide) (PEO) and poly(vinly alchol) (PVA), show a poor cellular viability without modification with cell adhesive proteins or peptides, such as collagen, laminin, fibronectin, and the RGD sequence [7, 8]. On the other hand, cell-adhesive proteins purified from living tissues induce some drawbacks, such as high cost, quality change induced by different batches, risk of virus infection, etc. To overcome these drawbacks, we have tried to find synthetic hydrogels that can directly promote cell adhesion and proliferation, with no need of surface modification by any cell-adhesive proteins or peptides. As a result, we found that cells can adhere, spread and proliferate on negatively charged synthetic hydrogels, with no protein modification on their surfaces. Furthermore, we found that the cell behavior is related to the chemical structure and Zeta potential (ζ) of the synthetic hydrogels [9]. In addition, immune response and toxicity of the high-strength double network (DN) hydrogel have been investigated, which showed that DN gels combined of various synthetic polymers, such as PAMPS(poly(2-acrylamido-2-methyl-propane sulfonic acid))/ PDMAAm(polydimethyl acrylamide), PAMPS/PAAm(polyacrylamide) are better than

DN gels combined of synthetic polymers and nature polymer, such as bacteria cellulose/PDMAAm or DN gels that combined of two kinds of nature polymers, such as bacteria cellulose/gelatin[10]. Excellent cellular compatibility as well as biological responses of negatively charged synthetic hydrogels would substantially promote the application of hydorgels for tissue engineering.

3.1 EC adhesion, spreading, and proliferation on various kinds of hydrogels

The hydrogels that we evaluated were neutral polymers, such as poly(vinyl alcohol) (PVA) and polyacrylamide (PAAm); weak polyelectrolytes with pH-dependent dissociated charged groups, such as poly(acrylic acid) (PAA) and poly(methacrylic acid) (PMAA) that are both having carboxylic acid groups on the side chains of the polymers; as well as strong polyelectrolyte with charged groups fully dissociated, such as poly(2-acrylamido-2-methyl-propane sulfonic acid sodium salt) (PNaAMPS) and poly(sodium p-styrene sulfonate) (PNaSS), both having sulfonate groups on the side chains of the polymers.

Figure 1 shows the phase-contrast micrographs of bovine fetal aorta endothelial cells (BFAECs) cultured on the protein-free hydrogels with various chemical structures. As shown in Figure 1, at the initial stage (6 h, column I), the chemical structure of the hydrogels do not have a remarkable influence on the BFAEC adhesion. However, after a prolonged culture time (120 h, column II), cell morphology strongly depends on the charge of the gels. Cells proliferate to reach confluency on strong polyelectrolyte gels (PNaSS, PNaAMPS), and hardly proliferate on neutral gels (PVA), while on weak polyelectrolyte (PAA, PMMA), the cells only modestly increase, in between neutral and strongly charged gels.

The proliferation kinetics of BFAECs on various kinds of hydrogels is shown in Figure 2. Except on PAAm gel, BFAECs exhibit proliferation on the PVA, PAA, PMAA, PNaSS, and PNaAMPS hydrogels. The BFAEC proliferation is the fastest on the strong polyelectrolyte

gels, PNaSS and PNaAMPS, and the proliferation rate on these hydrogels is very near to that on collagen hydrogel. The BFAEC proliferation rate on the weak polyelectrolyte gels, PAA and PMMA, is lower than that on the strong polyelectrolyte gels. The BFAECs proliferate to confluency on the PNaSS and PNaAMPS hydrogels with a cell density higher than 1.1×10^5 cell/cm^2 at 144 h. In the *in vivo* vascular systems, the inner surface of blood vessel is covered by a continuous EC monolayer, thus, EC proliferation *in vitro* is important for forming a continuous monolayer of cells on artificial blood vessels made from gels.

We have further found that the cell adhesion, spreading and proliferation depend not only on the chemical structure but also on cross-linker concentration *M* of the gel. Figure 3 shows results on the morphology of BFAECs cultured on PVA, PAAm, PAA, PMAA, PNaSS, and PNaAMPS hydrogels with various *M* at the initial culture time (6 h after seeding of cells on the gels) (Figure 3a) and the density of cells that proliferate to confluency or sub-confluency on these gels at a prolonged culture time (168 h after seeding of cells on gels) (Figure 3b). As shown in Figure 3a, all gels show substantially high cell adhesion, and the sum of the adhesive ratio (the number percentage of cells that more or less stick tightly to gel but remain spherical shape) and spreading ratio (the number percentage of cells that adhere on hydrogel with a change to fusiform or polygonal shape, concomitant with extension of pseudopodia) is higher than 50 % [11]. The results show that at the initial stage, the chemical structure and *M* of gels do not have a remarkable influence on cell adhesion. However, the chemical structure and *M* of gels obviously affect the spreading ratio and cell density after a long time of culture (120 h). For example, the spreading ratio on the PVA hydrogel is about 50 %, when *M* is 6 and 10 mol%, and the spreading BFAECs proliferate with culture time and reach sub-confluent at 168 h, with a cell density of 3.72×10^4 and 2.67×10^4 cell/cm^2, for 6 and 10 mol%, respectively (Figure 3b). While the spreading ratio decreases to about 15 % when *M* is 2 and 4 mol%, and the BFAECs do not proliferate with culture time.

The *M* dependence of spreading and proliferation behavior of cells is also observed for the

weakly-charged PAA and PMAA gels. On the other hand, no distinct difference in cell behaviors is observed on the strongly-charged PNaSS and PNaAMPS gels. The BFAECs can adhere, spread, and reach confluent on the PNaSS and PNaAMPS gels over a wide range of *M* (Figure 3).

The results indicate that cell proliferation is very sensitive to the chemical structure and hydrophobic/hydrophilic properties of weakly-charged hydrogels. It was reported that carboxylic acid groups of the PAA-grafted surface have a negative effect on cell adhesion, spreading, and growth [12]. Other researchers have showed that there were only a few cells attached onto PAA-grafted surface, and cell proliferation was very slowly [13]. Our results indicate that if the PAA is cross-linked at a suitable condition, the PAA hydrogel is favorable to cell adhesion and cells further proliferate to a confluent cell monolayer.

It is interesting to notice that cell spreading ratio on the PNaAMPS hydrogel (M = 6 mol%) at 6 h is only 16.2 % (Figure 3a), however, BFAECs proliferate normally and reach confluency with a prolonged culture time (Figure 3b).

With the change of the cross-linker concentration, the water content of the gel and the elastic modulus E of the gel are changed. Next, we discuss the effects of water content and elasticity of the gels, two key parameters for soft and wet gels. The water content of a gel is usually expressed in terms of swelling degree q, which is defined as the volume ratio of the swollen gel to the dried gel. Table 1 shows the swelling degree of the gels prepared at various cross-linker concentrations. The quite different q for the same cross-linker M is due to the different reactivity of the monomer species. As shown in Figure 4a, we could not find a clear correlation between the cell density and the swelling degree q. Furthermore, according to scaling theory, the elastic modulus E and the swelling degree q obey a scaling relationship of $E \sim q^{-3}$ for a non-charged gel with its partial chains in a Gaussian distribution[14]. We have recently found that when the charged gels are swelling in aqueous solutions with a high ionic strength, such as the HEPES buffer solution (ionic strength I=0.15) or sea water

(I=0.7)[15],whereupon the osmotic swelling term of the dissociated counter-ions is screened, they also, approximately, obey the relation of $E \sim q^{-3}$ of the neutral gel. Therefore, we can assume that the behaviors of the cells are also not correlated to the elastic modulus of the gels in the present case. This is in agreement with the literature results that the cell proliferation increased when the Young's modulus increased from ~1 kPa to ~10 kPa [16]. When the Young's modulus was higher than ~10 kPa, gel stiffness did not obviously affect cell proliferation. Our study also showed that cell proliferation did not obviously change when the Young's modulus of hydrogels increased from ~10 kPa to ~200 kPa (not published data). In this work, the most soft gel was 1 mol% PVA which had a Young's modulus of 52.6 kPa, more than 5 times higher than 10kPa, therefore, we considered that cell proliferation is not affected by gel stiffness in this study.

The above study suggests that cell adhesion, spreading and proliferation correlate to the charge density of hydrogels. Therefore, the Zeta potential (ζ) of the PAAm, PVA, PAA, PMAA, PNaSS, and PNaAMPS hydrogels were measured, to analyze the effect of surface charge density on cellular viability. Figure 4b shows Zeta potential (ζ) of gels as a function of swelling degree q of the gels in HEPES buffer solution. Even for the neutral PVA gel, it has a slightly negative Zeta potential, and $|\zeta|$ decreased with the increase in the q. The strong polyelectrolyte gels, PNaSS and PNaAMPS, showed a high negative value of the Zeta potential, and the value of $|\zeta|$ was almost independent on q. On the other hand, the weak polyelectrolyte gel, PAA and PMAA, showed an increase in $|\zeta|$ value with the increase in q. It indicates that ionization of carboxylic acid groups of weakly charged hydrogel increases with increasing swelling degree q. This is because the mesh size of hydrogel increases with increasing q, results in an increase in the distance between polymer chains. For maintaining a thermodynamically stable state in a small space, ionization of carboxylic acid groups of the PAA and PMAA hydrogels is enhanced due to decreased electrostatic repulsion in the hydrogel network. We can theoretically estimate the surface charge density of the polyelectrolyte gel.

For a strong polyelectrolyte gel carrying one charge at each repeated unit, the bulk counter-ion concentration c_e (m^{-3}) is related to the swelling degree q (g/g) of the gel as[17]

$$c_e = \frac{10^6 N_A}{qM_W} \qquad (1)$$

Here, N_A is the Avogadro number, and M_w (g/mol) is the molar weight of the polymer repeat unit. Supposing that the surface charge density of the gel is $\sigma_e = (c_e)^{2/3}(\mathrm{m}^{-2})$, then

$$\sigma_e = (\frac{10^6 N_A}{qM_W})^{2/3} \qquad (2)$$

Using $M_w = 229$ g/mol for PNaAMPS, the counter-ion density of the bulk PNaAMPS gel was calculated as $c_e = 2.6q^{-1}nm^{-3}$, and the surface counter-ion density of gel was calculated as $\sigma_e = 1.9q^{-2/3}$ nm^{-2}. So, the charge density for the PNaAMPS gel with q=20, for example, is 0.26 nm^{-2}. The constant Zeta potential of the strong polyelectrolyte gels, PNaSS and PNaAMPS, is probably related to the counter-ion condensation effect [18-20].

To find the correlation between the Zeta potential and the cell viability, we plot the cell density against the Zeta potential, as shown in Figure 4c. We found that although the gels have a different charge density, so long as they have a negative ζ higher than *c.a.* $20\,mV$, they facilitate cellular viability at the environment of serum containing medium. For example, when the *M* of the PAA hydrogel is 1 and 2 mol%, which show cell spreading and proliferation, ζ is -26.5 and -28.4 mV, respectively (Figure 4c).

The ζ of PNaAMPS (-25 ~ -30 mV) and PNaSS (-20 mV) in HEPES buffer solution does not obviously change with cross-linker concentration (Figure 4b) due to the fully dissociated nature of the strong polyelectrolyte. This is in agreement with the result of the BFAEC proliferation on the PNaAMPS and PNaSS gels, which is not sensitive to the cross-linker concentration. These results suggest that the ζ of gel in the range of about -30 ~ -20 mV is suitable for BFAEC proliferation, regardless of their different chemical structures.

3.2 EC adhesion, spreading and proliferation on copolymer hydrogels

Taking advantage of the above result, we systematically controlled the cell behavior by changing the charge density of gels using copolymerized gels from charged monomer and

neutral monomer. Three kinds of cells, i.e., BFAECs, human umbilical vein endothelial cells (HUVECs), and rabbit synovial tissue-derived fibroblast cells (RSTFCs), on poly(NaAMPS-co-DMAAm) hydrogels with various charge density were investigated [21]. The charge density of the copolymer gels was quantitatively tuned by adjusting the molar fraction, *F*, of negatively charged monomer in copolymer hydrogels.

Figure 5 shows the phase-contrast micrographs of BFAECs (column I), HUVECs (column II), and RSTFCs (column III) cultured on poly(NaAMPS-co-DMAAm) hydrogels with various molar fraction, *F*, at a cultivation time of 120 h. Figure 6 shows cell density of the three kinds of cells at 120 h as a function of molar fraction *F* of poly(NaAMPS-co-DMAAm) gels. The figures show that cell morphology and density are sensitive to *F* (or the Zeta potential ζ) and there is a critical *F* (or ζ) controls cell adhesion and proliferation.

There is a critical ζ = -20 mV (*F* = 0.4) for BFAECs and HUVECs initial spreading and proliferation. While the critical ζ for RSTFCs shifts to ζ = -28.5 mV (*F* = 0.7) (Figure 6). The results indicate that the critical ζ, slightly depends on cell variety. We suppose that the difference originates from the adhesive proteins and cell membrane receptors for attachment of different kinds of cells to PNaAMPS-based gel scaffolds.

3.3 Correlation between protein adsorption and cell proliferation

The question is why cells spread and proliferate on protein-free hydrogel surface with a ζ lower than $-20\,mV$. Because the cell surface is negatively charged, hydrogels that show increased cellular viability are negatively charged also, therefore, direct electrostatic interaction between the ECs and gels cannot explain the phenomenon. It is well known that adhesive proteins play an important role in the process of cell spreading and proliferation[22]. Proteins are amphoteric polyelectrolyte with both acidic and basic peptide that behaves as a bridge between positive or negative groups on the EC or gel surface. Therefore, we

considered that serum proteins contained in the culture medium might interact with the negatively charged gel by electrostatic interactions, and act as the bridges. To elucidate this, we further investigated the effect of Zeta potential (ζ), i.e., charge density, on the amount of total adsorbed proteins from serum containing culture medium, and the fibronectin contained in the total adsorbed proteins on the poly(NaAMPS-co-DMAAm) gels [21]. Fibronectin adsorption has been studied extensively because the adsorbed fibronectin on substrates plays an important role in stimulating cell adhesion, spreading, growth and migration [23, 24].

Figure 7 shows the amount of total adsorbed proteins and the fluorescence intensity of fibronectin on the poly(NaAMPS-co-DMAAm) hydrogel surfaces as a function of ζ [21]. When $\zeta \geq$ -20 mV ($F \leq 0.4$), the concentration of total adsorbed proteins and the intensity of fibronectin slowly increase, while when ζ = -20 mV (F = 0.4) the concentration of adsorbed proteins and the intensity of fibronectin begin to dramatically increase. It is interesting to note that when $\zeta \leq$ -20 mV ($F \geq 0.4$), the intensity of fibronectin continuously increases while the concentration of total adsorbed proteins does not change. It indicates that fibronectin preferentially adsorbs from the serum containing culture medium onto the copolymer gels with a decrease of ζ. The effects of ζ on total proteins and fibronectin adsorption coincide well with cell behavior. The results indicated that hydrogel charge density adjusts protein adsorption, i.e., more negative charge, more protein adsorption, which favors cell spreading and proliferation.

4. Platelet adhesion on cultured ECs

The ideal artificial blood vessel should have a structure similar to *in vivo* blood vessels and take full advantages of cell functions. The inner surface of a blood vessel is covered by a functional EC monolayer which protects procoagulant activity [3, 4]. Therefore, an artificial blood vessel with EC monolayer on its inner wall is expected to inhibit thrombosis. Heparan sulfate proteoglycans (HSPGs), the main component of glycocalyx which is decorated on the

surface of EC monolayer, exhibit antithrombin activity [25, 26]. However, the blood compatibility of *in vitro* cultured ECs is poorly investigated [27]. It is doubtful that *in vitro* cultured ECs have the same anti-thrombogenic function as that of ECs *in vivo* [28]. Thus, we designed experiments to understand human platelet adhesion to HUVECs cultured on various kinds of chemically cross-linked anionic hydrogels. The study discovers, for the first time to the authors' knowledge, that the HUVECs cultured on the protein-free PNaAMPS and PNaSS gels show excellent platelet compatibility, especially on the PNaSS hydrogel. Furthermore, the platelet compatibility was enhanced when the HUVECs were treated with transforming growth factor β_1 (TGF-β_1), which stimulates synthesis of HSPGs on the HUVECs surface, whereas the platelet compatibility was decreased when the HUVECs were treated with heparinase I, which disrupt HSPGs, indicating that the different platelet adhesion properties are attributed to the amount of glycocalyx on the HUVECs cultured on different kinds of gel scaffolds.

4.1 Platelet adhesion on the ECs cultured on various kinds of hydrogels

The morphology of the adhered platelets (spherical shape, spreading shape, and pseudopodia extension) as observed by scanning electron microscope (SEM) images is one of the indexes expressing the degree of the platelet activation [29, 30]. A large amount of platelets adhere on the bare poly(ethylene terephthalate) (PET) plate (271 cells /$10^4\mu m^2$), and 53.9% of all adhered platelets are spreading, 43.1% platelets are rounded with pseudopodia extension, indicating the activation of the platelets (Figure 8) [31]. Except on the bare PET plate, the platelets that adhere on the cultured HUVECs and on the bare polystyrene (PS) plate keep their original spherical shape, indicating not activate of the platelets. The density of adhered platelets on the HUVEC sheet cultured on the PS plate (185 cells/$10^4\mu m^2$) is obviously lower than that on the bare PS plate (320 cells /$10^4\mu m^2$). It shows that the HUVEC sheet cultured on the PS plate inhibits platelet adhesion comparing with the bare PS plate.

The density of adhered platelets on the as-prepared HUVECs cultured on PAA hydrogels is 115 cells/ $10^4\mu m^2$, and not dependent on the *M* of the hydrogel (Figure 9) [31]. When the *M* of PNaAMPS hydrogel is 2, 4, and 10 mol%, the density of adhered platelets on the as-prepared HUVEC monolayers is 183, 34, and 6 cells/$10^4\mu m^2$, respectively. It shows that the platelet adhesion on the HUVEC monolayers cultured on the strong anionic PNaAMPS hydogels decreases with increasing the *M* of the gel. It is a surprising result that no platelets adhere on the HUVEC monolayers cultured on the PNaSS gels, regardless of the *M* (4 and 10 mol%) of the gels.

The above results demonstrated that the anti-platelet adhesion of the HUVECs cultured on various scaffolds increases in the order of PS<PAA<PNaAMPS<PNaSS, indicating that the platelet compatibility of the HUVECs cultured on these anionic hydrogels is higher than that of PS plate. In addition, the ability of platelet adhesion on HUVECs depends on the chemical structure and cross-linker concentration of the gels used as scaffolds for HUVEC cultivation.

4.2 Glycocalyx affects platelet adhesion

We hypothesized that the glycocalyx on the surface of the endothelial cells, was affected by the chemical and physical properties of the gel scaffolds because platelet adhesion closely correlates to the glycocalyx. To verify this, we modulated the glycocalyx on the cultured HUVECs, and studied its influence on the platelet compatibility [31].

We have found that after the treatment of HUVEC surface using TGF-β_1, a growth factor to stimulate the production of HSPGs, the density of adhered platelets on the HUVECs cultured on the PAA hydogel dramatically decreased from to 115 to ~10 cells/$10^4\mu m^2$, for 1 and 2 mol% cross-linker concentrations. The density of adhered platelets on the HUVEC monolayer cultured on PNaAMPS gel dramatically decreases from 183, 34 cells/$10^4\mu m^2$ to 15, 17 cells/$10^4\mu m^2$, respectively, for 2 and 4 mol% cross-linker concentration. The density of adhered platelets on the HUVEC monolayer cultured on the 10 mol% PNaAMPS gel was 6

cells/$10^4\mu m^2$, and it does not change by TGF-β_1 treatment. On the other hand, after the treatment of the HUVECs with heparinase I, a enzyme that removes the HSPGs, the density of adhered platelets on the HUVEC monolayer cultured on the PNaSS hydrogel increased from 0 to 87 and 32 cells/$10^4\mu m^2$, respectively, for 4 and 10 mol% cross-linker concentration. The results demonstrate that for the *in vitro* cultured HUVECs exhibiting a large amount of platelets adhesion, after they are treated by TGF-β_1, i.e., increase the amount of HSPGS, platelet adhesion obviously decreases comparing with the as-prepared HUVECs. On the other hand, for the cultured HUVECs that do not show platelet adhesion, after they are treated by heparinase I, i.e., decrease the amount of HSPGS, platelets begin to adhere on the HUVECs. Therefore, the amount of glycocalyx on the cultured HUVECs modulates platelet adhesion. Our result is in agreement with animal experiments that demonstrated platelet adhesion was induced when the EC glycocalyx of vein of Golden hamsters was degraded by oxidized lipoproteins [32]. These results demonstrate that it is possible to fabricate hybrid artificial blood vessel with high blood compatibility from PNaAMPS and PNaSS hydrogels with ECs monolayer on their inner surfaces. On the basis of this study, we proposed that a material that only favors cell proliferation is not suitable enough for use in tissue engineering. As an ideal material for tissue engineering, it should not only favor cell proliferation but also maintain the original functions of the cells.

5. Application of hydrogel in tissue engineering

5.1 Selective EC adhesion and proliferation on micro-patterned hydrogel surfaces

Cell behavior in complex tissues where available space is limited, such as in branching capillary vessel network, is still not well understood [33, 34]. In fact, not only chemical properties, but also topographical patterns of substrates can influence cellular responses, because cell growth, morphology, viability, and gene expression are remarkably influenced by micro-patterns on substrates. In most cases, micro-patterns have been fabricated on rigid

surfaces, such as glass and titanium, or on polymer coated substrates [35, 36]. However, the elasticity of these rigid substrates is far different from the ECM of living body which has elastic moduli only in the order of 10 to 10^4Pa [37]. It is considered that cell behavior on soft and wet substrate is more similar to that in living body comparing with that on hard and dry scaffolds. For studying the effect of the viscoelasticity of micro-patterned hydrogel substrate on cell behavior, designing and fabricating micro-patterned hydrogel surfaces are crucially important.

We developed a laser beam polymerization method to fabricate stable micro-patterned hydrogel substrate [38]. The basic idea is that we first prepared a neutral gel, such as PAAm, that does not show cell viability. Then, we immersed the gel in a charged monomer solution, such as NaAMPS. Finally, we use a UV laser beam to initiate the polymerization of the charged monomer to obtain a strip-like double network structure. The straight and curved stripes are successfully fabricated during polymerization of PNaAMPS which can support cell proliferation, in a PAAm hydrogel substrate which cannot support cell proliferation. The micro-patterned hydrogel is named PNaAMPS/PAAm. Figure 10 shows the phase contrast micrographs of BFAECs cultured on the PNaAMPS/PAAm micro-patterned hydrogel surfaces with 11μm and 23 μm-wide straight stripes, as well as 11μm-wide curved stripe fabricated by the laser beam polymerization method [38]. The BFAECs selectively adhere on micro-patterned PNaAMPS surface and spread very well in a fusiform shape, aligning along the stripes. Decreasing the width of the PNaAMPS strips increases the degree of anisotropic spreading of cells and the degree of cell orientation, as characterized by the aspect ratio of the length of the longest axis to the width of cells (Figure 11). The degree of cell alignment can also be characterized as the angle between the stripe verge of the micro-patterns and the longest axis of the cells. A small angle represents the high degree of cell alignment. The cells with the angle lower than 10° are considered as aligning along the patterns. Figure 12 shows the ratio of aligned BFAECs as a function of angles on micro-patterned PNaAMPS/PAAm

hydrogel stripes with various width of the strip for cells cultured for 24 h [38].

These results demonstrate that the morphology of ECs changes from a polygonal to a fusiform shape and to be uniformly oriented in the direction of the long axis of micro-patterned stripes, when the width of stripe is close to the size of the cells. Subjecting ECs to fluid shear stress show similar shape transformation [39], considered together, not only fluid shear stress but also geometric limitation can modulate cell shape and direction.

5.2 EC adhesion and proliferation on tough hydrogels

In physiological condition, many tissues, such as articular cartilage, semilunar cartilage, tendons, ligaments, and blood vessel exist in a severe mechanical dynamic environment. Accordingly, these living tissues, containing 50-80 wt% water, are soft and wet materials with an excellent mechanical property: They have the elasticity in a range of several 100 kPa to MPa, and sustain deformations as large as 100 % and failure stresses of 1-10 MPa. Furthermore, the role of tissue cells is important in biological activity. Therefore, from a potentially practical view point, in order to replace natural tissues with hydrogels, design and production of hydrogels that satisfy several critical parameters at the same time, such as high level of cellular viability and high mechanical strength, are crucially important for the biomedical applications of hydrogels.

Recently, we developed a general method to obtain tough hydrogels by inducing a double-network (DN) structure that combines various kinds of hydrophilic polymers [40-44]. The DN hydrogels consist of two interpenetrated polymer networks: one is made of highly cross-linked negatively charged polymers (as rigid first network) and the other is made of loosely cross-linked neutral polymers (as flexible second network). The DN hydogels, containing about 90 wt% water, possess hardness (elastic modulus of 0.3 MPa), toughness (fracture stress of ~20 MPa), and excellent wear property [40]. Adjusting components of the first and second network of DN hydrogels can independently control these quantities. This is convenient for practical application.

However, the usual tough DN hydrogels, such as PNaAMPS/PDMAAm, PNaAMPS/ PAAm, do not facilitate cell spreading and proliferation, although many cells can adhere to the surfaces of these hydrogels. This is because in the process of DN synthesis, the second monomer mostly polymerizes on the surface of first network, therefore, the surface chemical composition and the properties of DN hydrogels are determined by the second component, that is, the neutral component, such as PDMAAm and PAAm, which is not suitable for cell spreading and proliferation.

As previously described, BFAECs can spread, proliferate, and reach confluent or sub-confluent on synthetic hydrogels with negative charges, such as PNaAMPS, PNaSS, and PAA hydrogels [9, 11, 30]. Taking the advantages of these previous works, gels with triple network (TN) structure of charge/neutral/charge networks with both high mechanical strength and cell viability have been synthesized. For example, PNaAMPS/PDMAAm/ Poly(NaAMPS-co-DMAAm) TN gel consists of charged moiety PNaAMPS as the first network, neutral moiety DMAAm as the second network, and their copolymer poly(NaAMPS-co-DMAAm) (F = 0.5) as the third network shows fracture stress as high as 1 ~ 3 MPa, much higher than the single network gels of PNaAMPS (0.63 MPa) and poly(NaAMPS-co-DMAAm) (F = 0.5) (0.26 MPa) (Table 2) [21]. Figure 13 shows the BFAEC densities on the TN hydrogels as a function of culture time. On PAMPS/PDMAAm DN hydrogel and TN hydrogel that the third network is not cross-linked (sample TN-0), no cell spreading is observed. It is considered that the high mobility of the polymer chains does not facilitate cell spreading and proliferation [31].

When the third network cross-linker concentration is 2 and 4 mol%, BFAECs proliferate and reach confluent. It also shows that the BFAEC proliferation rates on TN-2 and TN-4 hydrogels, and the cell densities at 120 h on the TN-2 (1.0×10^5 /cm^2) and TN-4 hydrogels (1.1×10^5 /cm^2) are similar to that on poly(NaAMPS-co-DMAAm) (F = 0.5) single network hydrogel (1.4×10^5 /cm^2) [21]. These results indicated that the surface properties of the TN

hydrogels with poly(NaAMPS-co-DMAAm) as the third component are similar to that of the single network poly(NaAMPS-co-DMAAm) hydrogel. A slightly slow cell proliferation rate on TN hydrogels compared with that on poly(NaAMPS-co-DMAAm) (F = 0.5) hydrogel is observed, and it is attributed to the slightly higher ζ of TN hydrogels than that of poly(NaAMPS-co-DMAAm) (F = 0.5) gel.

These TN hydrogels are thermally and chemically stable, they do not show any change in mechanical strength even after higher temperature sterilization (120 °C) in HEPES buffer solution and after cell cultivation. The results will substantially promote the application of tough hydrogels as scaffold for soft and wet tissues. Furthermore, the general concept of regulating cell proliferation by charge density may be broadly applicable to design and select proper polymer materials in tissue engineering applications.

6. Concluding remarks

We found that although negatively charged synthetic hydrogels, such as PAA, PMAA, PNaSS, and PNaAMPS have different chemical structures and charge density, so long as they have a Zeta potential (ζ) lower than *c.a.* -20 mV, they can directly promote cell adhesion and proliferation, with no need of surface modification by any cell-adhesive proteins or peptides at the environment of serum containing medium.

Taking advantage of the above result, we systematically controlled cell behavior by changing the charge density of gels using copolymerized gels from charged monomer and neutral monomer. There is a critical ζ = -20 mV for two kinds of ECs (BFAECs and HUVECs) proliferation, while the critical ζ for RSTFCs shifts to ζ = -28.5 mV, which is about 8 mV lower than that of ECs, indicating that the critical ζ slightly depends on cell variety. In addition, the effect of gel charge on cell behavior is correlated well with the total proteins and fibronectin adsorption. The above concept of regulating cell proliferation by charge density may be broadly applicable to design and select proper polymer materials in tissue engineering

applications.

The antithrombin activity of HUVEC monolayer cultured on hydrogels was further investigated, and it was found that the HUVECs cultured on the protein-free PNaAMPS and PNaSS gels show excellent platelet compatibility, especially on the PNaSS hydrogel. In contrast, a large amount of platelets adhered on the HUVEC monolayer cultured on the PS plate. Furthermore, the platelet compatibility was enhanced when the HUVECs were treated with transforming growth factor β_1 (TGF-β_1), which stimulates synthesis of HSPGs on the HUVECs surface, whereas the platelet compatibility was decreased when the HUVECs were treated with heparinase I, which disrupt HSPGs, indicating that the different platelet adhesion properties are attributed to the amount of glycocalyx on the HUVECs cultured on different kinds of gel scaffolds. On the base of the study, we propose a material that only favors cell proliferation is not suitable for use in tissue engineering. As an ideal material for tissue engineering, it should not only favor cell proliferation but also maintains the original cell functions.

Further studies, such as developed micro-patterned hydrogels for cell selective spreading, proliferation, and orientation on the micropatterned, synthesizing hydrogels with both high mechanical strength and cell viability at the same time, have been performed, which will promote the potential applications of synthetic hydrogels in tissue engineering.

The new insight in finding synthetic polymer hydrogels which control cell adhesion and proliferation, suitable for cells maintaining their original functions, and have sufficient mechanical strength at the same time, will open a new era of soft and wet materials as substitutes for tissue engineering.

Acknowledgment

This research was financially supported by a Grant-in-Aid for Specially Promoted Research (No. 18002002) from the Ministry of Education, Science, Sports and Culture of Japan.

References

[1] Osada, Y., Kajiwara, K., *Gels Handbook*, (Academic Press, New York, 2001).

[2] Osada, Y., *Handbook of Biomimetics*, (Academic Press, New York, 2000).

[3] Pries, A.R., Secomb, T.W., Jacobs, H. *Am. J. Physiol.* **273**, H2272-2279 (1997).

[4] Vink, H., Constantinescu, A.A., Spaan, J.A.E. *Circulation* **101**, 1500-1502 (2000)

[5] Forsey, R.W., Fisher, J., Thompson, J., Stone, M.H., Bell, C., Ingham, E., *Biomaterials*, **27**, 4581-4590 (2006).

[6] Sun, Y., Berger, E. J, Zhao, C., Jay, G. D., Kai-Nan A. N., Amadio P. C., *J. Orthop. Res.* **24**, 1861-1868 (2006).

[7] Schmedlen, R. H., Masters, K. S., West, J. L., *Biomaterials*, **23**, 4325-4332 (2002).

[8] Chung, T. W., Lu, Y. F., Wang, S. S., Lin, Y. S., Chu, S. H. *Biomaterials*, **23**, 4803-4809 (2002)

[9] Chen, Y. M., Gong, J. P., Osada, Y., Gel: a Potential Materials as Artificial Soft Tissue, In *Macromolecular Engineering: Precise Synthesis Materials Properties, Applications*, eds. Matyjaszewski, K., Gnanou, Y., Leibler, L., (Wiley-VCH, 2006), Chap. 17 , pp. 2689-2717

[10] Tanabe, Y., Yasuda, K., Azuma, C., Taniguro H., Onodera S., Suzuki A., Chen, Y. M., Gong, J. P., Osada, Y., *J. Mater. Sci: Mater. Med.* **19**, 1379-1387, (2008).

[11] Chen, Y. M., Shiraishi, N., Satokawa, H., Kakugo, A., Narita, T., Gong, J. P., Osada, Y., Yamamoto, K., Ando, J., *Biomaterials* **26**, 4588-4596 (2005).

[12] Lee, J. H., Lee, J. W., Khang, G., Lee, H. B., *Biomaterials*, **18**, 351-358 (1997).

[13] Lee, S. D., Husiue, G. H., Chang, P. C. T., Kao, C. Y., *Biomaterials* **17**, 1599-1608 (1996).

[14] de Gennes PG. 1979. Scaling concepts in polymer physics. Ithaca: Cornell University Press.

[15] T. Murosaki, T. Noguchi, A. Kakugo, A. Putra, T. Kurokawa, H. Furukawa, Y. Osada, J. P. Gong, Y. Nogata, K. Matsumura, E. Yoshimura & N. Fusetani, *Biofouling*, **25**, 313-320(2009).

[16] Yeung T, Georges PC, Flanagan LA, Marg B, Ortiz M, Funaki M, Zahir N, Ming W, Weaver V, Janmey PA. *Cell Motility Cytoskeleton* **60**, 24-34(2005)

[17] S. Oogaki, G. Kagata, T. Kurokawa, S. Kuroda, Y. Osada, and J. P. Gong, *Soft Matter*, in press.

[18] F. Oosawa, *J. Polym. Sci.* **23**, 421(1957).

[19] G. S. Manning, *J. Chem. Phys.* **51**, 934(1969).

[20] G. S. Manning, *J. Phys. Chem.* **79**, 262(1975).

[21] Chen, Y. M., Gong, J. P., Tanaka, M., Yasuda, K., Yamamoto, S., Shimomura, M., Osada, Y., *J. Biomed. Mater. Res.* **88A**: 74-83 (2009)

[22] Ratner, B.D., Bryant S. J., *Annu. Rev. Biomed. Eng.* **6**, 41-75(2004).

[23] Calonder, C., Matthew, H. W. T., Tasse, P. R. V., *J. Biomed. Mater. Res.* **75A**, 316-23 (2005).

[24] Larsen, M., Wei, C., Yamada, K. M., *J. Cell. Sci.* **119**, 3376-3384 (2006).

[25] Weitz, J. I., *J. Clin. Invest.* **111**, 952-954 (2003).

[26] Segev, A., Nili, N., Strauss, B. H., *Cardiovas. Res.* **63**, 603-610 (2004).

[27] Woodsa, A. M., Rodenberga, E. J., Hilesb, M. C., Pavalkoa, F. M., *Biomaterials* **25**, 515-525 (2004).

[28] Chen, Y. M., Tanaka, M., Gong, J. P., Yasuda, K., Yamamoto, S., Shimomura, M., Osada,

Y., Biomaterials used for artificial blood vessels. JP Patent No.2006-141838 (2007)

[29] Tanaka, M., Motomura, T., Kawada, M., Anzai, T., Kasori, Y., Shiroya, T., Shimura, K., Onishi, M., Mochizuki, A., *Biomaterials*, **21**, 1471-1481 (2000).

[30] Tanaka, M., Motomura, T., Kawada, M., Anzai, T., Kasori, Y., Shimura, K., Onishi, M., Mochizuki, A., Okahata, Y., *Jpn. J. Artif. Organs.* **29**, 209-216 (2000).

[31] Chen, Y. M., Tanaka, M., Gong, J. P., Yasuda, Y., Yamamoto, S., Shimomura, M., Osada, Y., *Biomaterials*, **28**, 1752-1760 (2007).

[32] Vink, H., Constantinescu, A. A., Spaan, J. A. E., *Circulation*, **101**, 1500-1502 (2000).

[33] Curtis, A., Wilkinson, C., *Biomaterials*, **18**, 1573-1583 (1997).

[34] Flemming, R. G., Murphy, C. J., Abrams, G. A., Goodman, S. L., Nealey, P. F., *Biomaterials*, **20**, 573-599 (1999)

[35] Singhvi, R., Kumar, A., Lopez, G. P., Stephanopolous, G. N., Wang, D. I. C., Whitesides, G. M., Ingber, D. E., *Science*, **264**, 696 (1994).

[36] Chen, C. S., Mrksich, M., Huang, S., Whitesides, G. M., Ingber, D. E., *Science* **276**, 1425 (1997).

[37] Wakatsuki, T., Kolodney, M. S,. Zahalak, G. I., Elson, E. L., *Biophys J.* **79**, 2353-2368 (2000).

[38] Chen, Y. M., Shen, K. C., Gong, J. P., Yasuda, Y. *J. Nanosci. Nanotechnol.* **7**, 773-779 (2007).

[39]Tarbell, J. M., Pahakis, M. Y., *J. Intern. Med.* **259**, 339-350 (2006**)**.

[40] Gong, J. P., Katsuyama, Y., Kurokawa, T., Osada, Y., *Adv. Mater.***15**, 1155-1158 (2003).

[41] Nagayama, A., Kakugo, A., Gong, J. P., Osada, Y., Takai, M., Erata, T., Kawano, S., *Adv.*

Funct. Mater. **14**, 1124-1128 (2004).

[42] Yasuda, K., Gong, J. P., Katsuyama, Y., Nakayama, A., Tanabe, Y., Kondo, E., Ueno, M., Osada, Y., *Biomaterials*, **26**, 4468-4475 (2005).

[43] Kaneko, D., Tada, T., Kurokawa, T,. Gong, J.P., Osada, Y., *Adv. Mater.* **17**, 535-538 (2005).

[44] Azuma, C., Yasuda, K., Tanabe, Y. H., Kanaya, F., Nakayama, A., Chen, Y. M., Gong, J. P., Osada, Y., *J. Biomed. Mater. Res.* **81A**, 373-380 (2007).

[45] Narita, T., Hirai, A., Xu, J., Gong, J. P., Osada, Y., *Biomacromolecules,* **1**, 162-167(2000).

Figure captions

Figure 1　Phase-contrast micrographs of BFAECs cultured on various hydrogels at the initial stage (6h, column I) and at a prolonged culture time (120h, column II). Cross-linker concentration of hydrogels: PVA (6 mol%), PAA (2 mol%), PMAA (1 mol%), PNaSS (10 mol%), PNaAMPS (6 mol%). Scale bar: 100μm. (Reproduced with permission from the literature [11].)

Figure 2　Proliferation kinetics of BFAECs cultured on various kinds of hydrogels. (●) PVA (6 mol%), (♦) PAAm (4 mol%), (□) PAA (2 mol%), (○) PMAA (1 mol%), (Δ) PNaSS (10 mol%), (■) PNaAMPS (6 mol%). Error ranges are standard deviations over n = 4~8 samples. (Reproduced with permission from the literature [11].)

Figure 3 (a) Morphologies of BFAECs cultured on PVA, PAAm, PAA, PMAA, PNaSS, and PNaAMPS hydrogels with various cross-linker concentrations at 6 h. white bar: floating ratio, white bar with oblique lines: adhesive ratio, black bar: spreading ratio. (b) Density of cells that proliferate to confluent or subconfluent on various kinds of gels as a function of the cross-linker concentration. Error ranges are standard deviations over n = 4~8 samples. (Reproduced with permission from the literature [11].)

Figure 4　(a) Density of cells that proliferate to confluent or subconfluent on various kinds of gels as a function of swelling degree q. (b) Zeta potential (ζ) of hydrogels as a function of swelling degree (q) in HEPES buffer solution. (c) Density of cells that proliferate to confluent or subconfluent on various kinds of gels as a function of the Zeta potential. (▲) PVA; (□) PAA; (Δ) PMAA; (○) PNaSS; (◇) PNaAMPS. (Replotted from with permission from the literature [11].)

Figure 5 Phase-contrast micrographs of BFAECs (column I), HUVECs (column II), and

RSTFCs (column III) cultured on poly(NaAMPS-co-DMAAm) hydrogels with various molar fraction, F. Cultivation time:120 h. Scale bar: 100 μm. (Reproduced with permission from the literature [21].)

Figure 6 Cell density of three kinds of cells at 120 h as a function of molar fraction F of poly(NaAMPS-co-DMAAm) hydrogels. (□)BFAECs, (●)HUVECs, (○)RSTFCs. Error ranges are standard deviations over n = 4~8 samples. (Reproduced with permission from the literature [11].)

Figure 7 The amount of total adsorbed proteins (●) and fluorescence intensity of adsorbed fibronectin (■) on poly(NaAMPS-co-DMAAm) hydrogels as a function of Zeta potential (ζ) of hydrogels. Error ranges are standard deviations over n = 3~6 samples. (Reproduced with permission from the literature [21].)

Figure 8 The SEM images of the adhered platelets on the HUVECs cultured on various kinds of hydrogel and PS plate, as well as on bare PET and PS plates. The captions that have not ′bare′ indicate the cultured HUVEC surface. Column II and IV is the magnified images of Column I and III, respectively. Scale bar: 5μm. (Reproduced with permission from the literature [31].)

Figure 9 Densities of adhered platelets on un-treated, TGF-β_1 treated, and heparinase I treated HUVECs cultured on various kinds of substrates, and on bare PET and PS plates. The numbers in the figures are the cross-linker concentration of hydrogels. White bar: normal platelet with spherical shape, black bar: round platelet with pseudopode extension, white bar with oblique lines: spreading platelet. Error ranges are standard deviations over n = 3~5 samples. (Reproduced with permission from the literature [31].)

Figure 10 Phase contrast micrographs of BFAECs cultured on the PNaAMPS/PAAm micropatterned hydrogel surfaces fabricated by laser beam polymerization method. (a)Width

of the straight stripe is 11μm (upper) and 23 μm (lower). (b) Width of the curved stripe is 11μm, and the radius of curve is 245μm. Scale bar100 μm. (Reproduced with permission from the literature [38].)

Figure 11 Aspect ratio of the length of longest axis to the width of BFAECs cultured on the homogeneous PNaAMPS hydrogel with 4 mol% cross-linker (n = 50), and on the micropatterned straight stripes with width of 182 μm (n = 42), 23μm (n = 30), and 11μm (n = 7) when BFAECs proliferate to confluent. (Reproduced with permission from the literature [38].)

Figure 12 Ratio of BFAECs as a function of the angles between the stripe verge of the micropatterns and the longest axis of the BFAECs on the micropatterned PNaAMPS/PAAm straight stripes with wide of 182μm (n = 40), 23μm (n = 30), and 11 μm (n = 7) when cells were cultured at 24h. (Reproduced with permission from the literature [38].)

Figure 13 Densities of the BFAECs cultured on TN hydrogels with different cross-linker concentration of the third network, poly(NaAMPS-co-DMAAm) F = 0.5 (MBAA=4 mol%) as a function of culture time. (▲): 0 mol%, (●): 2 mol%, (Δ): 4 mol%. (■): poly(NaAMPS-co-DMAAm) F = 0.5 (4 mol%). Error ranges are standard deviations over n = 4~6 samples. (Reproduced with permission from the literature [21].)

Table 1 Degree of swelling *q* of various hydrogels used in this study in HEPES buffer solution ($NaHCO_3$ 1.55×10^{-2} M, HEPES 5×10^{-3} M, NaCl 0.14 M, pH = 7.4). Error ranges are standard deviations over n = 3~5 samples. PVA gel was cross-linked by glutaraldehyde from 5wt% polymer solution. Other gels were cross-linked by MBAA from their monomer solutions.

Table 2 Degree of swelling (q), elastic modulus (*E*), fracture stress (σ), and fracture strain (λ)

of PNaAMPS hydrogel (MBAA=4 mol%), poly(NaAMPS-co-DMAAm) F = 0.5 hydrogel (4 mol%), and TN hydrogels with various cross-linker densities in serum containing medium. Error ranges are standard deviations over n = 3~5 samples. (Reproduced with permission from the literature [21].)

Table 1

q / Hydrogel	Crosslinker concentration *M* (mol%)							
	1	2	3	4	5	6	8	10
PVA	13	7		5	–	3	–	2
PAAm	8.9±0.48	8.6±0.61	7.9±0.29	7.8±0.82	–	5.3±0.49	–	–
PAA	29.3±1.03	24.8±0.55	–	18.2±0.79	–	12.3±0.62	–	–
PMAA	24.6±0.77	19.97±.084	18.1±0.46	17.0±0.56	–	16.4±0.48	–	–
PNaSS	–	–	–	42.0±0.73	–	25.0±0.28	23.0±1.05	19.0±0.72
PNaAMPS	33.4±0.71	22.0±0.76	16.2±0.30	15.7±0.36	13.3±0.15	10.2±0.94	–	–

Table 2

Gels	First Network	Second Network	Third Network	q	E (MPa)	σ (MPa)	λ (mm/mm)
SN	PNaAMPS	–	–	17.0 ± 0.47	0.061 ± 0.33	0.63 ± 0.02	0.65 ± 0.04
	Poly(NaAMPS-*co*-PDMAAm) $F = 0.5$	–	–	12.2 ± 0.40	0.19 ± 0.01	0.26 ± 0.02	0.57 ± 0.02
TN	PNaAMPS	PDMAAm	Poly(NaAMPS-*co*-PDMAAm) $F = 0.5$				
			TN-0[a]	7.16 ± 0.25	0.32 ± 0.07	3.0 ± 0.52	0.71 ± 0.07
			TN-2[a]	6.98 ± 0.16	0.65 ± 0.13	2.31 ± 0.37	0.65 ± 0.09
			TN-4[a]	6.43 ± 0.16	0.88 ± 0.03	1.36 ± 0.31	0.47 ± 0.05

Error ranges are standard deviations over $n = 3$–5 samples.
[a]The numbers represent the cross-linker density in mole percent of the third network.

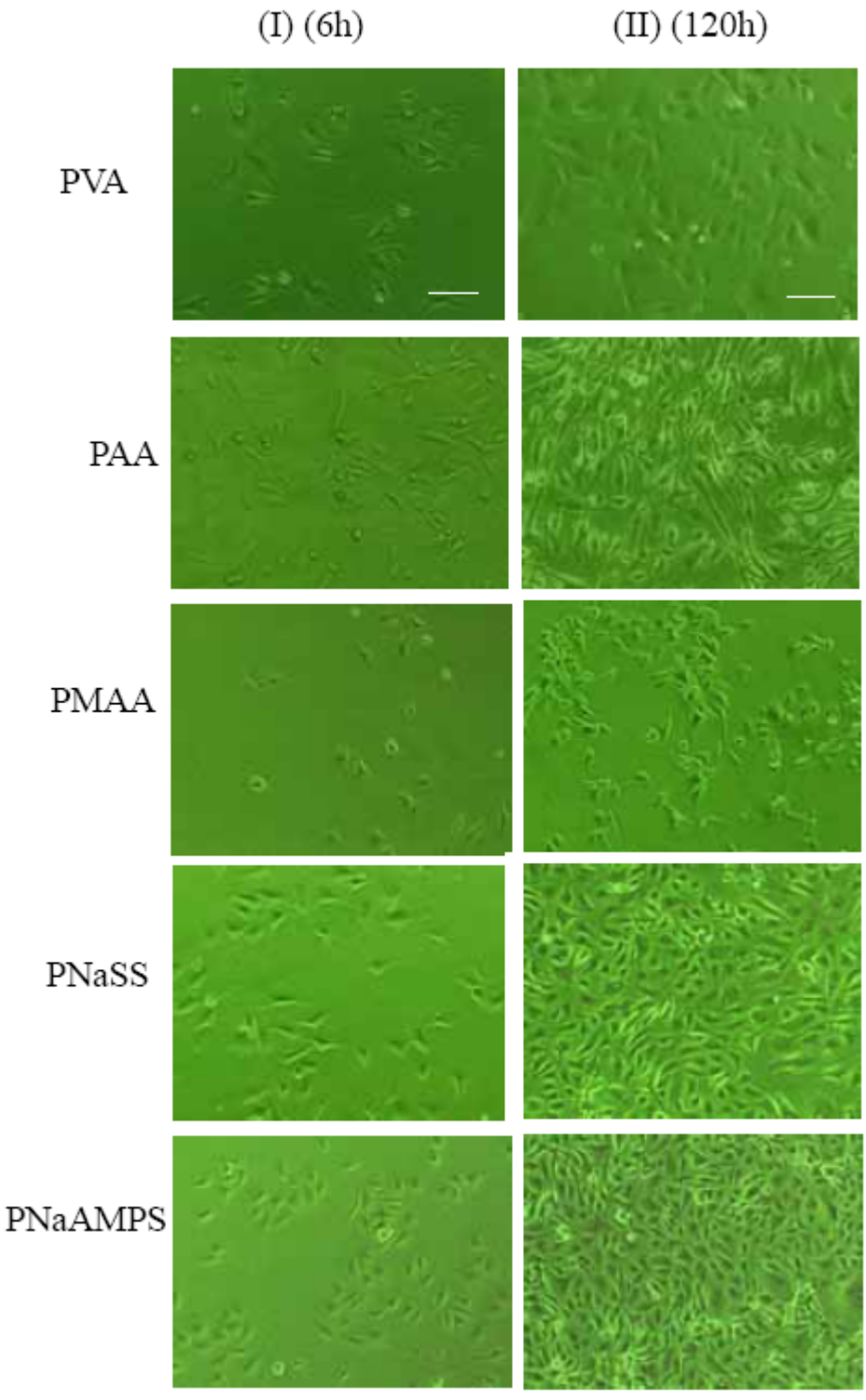

Figure 1

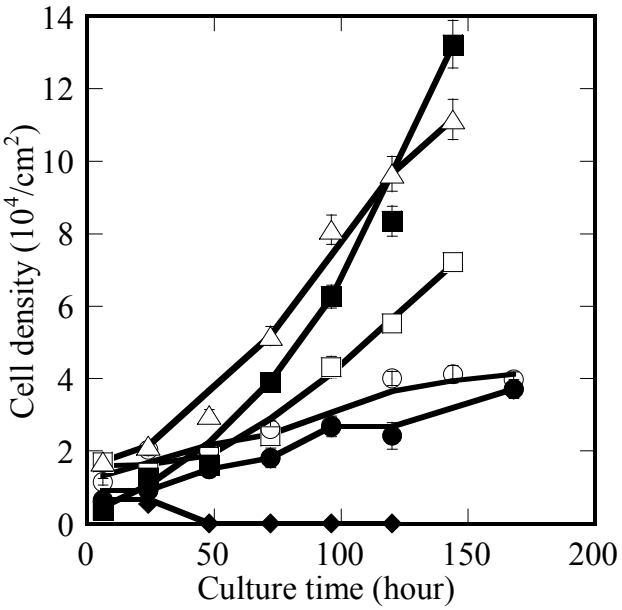
Cell density (10^4/cm^2)
Culture time (hour)
0
2
4
6
8
10
12
14
0
50
100
150
200

Figure 2

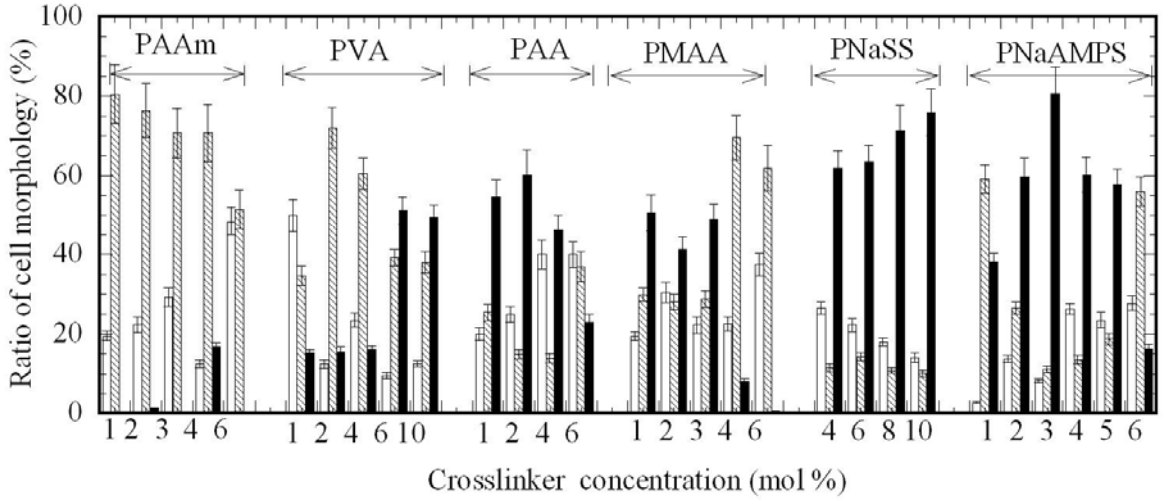
Ratio of cell morphology (%)
100
80
60
40
20
0
PAAm
PVA
PAA
PMAA
PNaSS
PNaAMPS
1 2 3 4 6
1 2 4 6 10
1 2 4 6
1 2 3 4 6
4 6 8 10
1 2 3 4 5 6
Crosslinker concentration (mol %)

Figure 3a

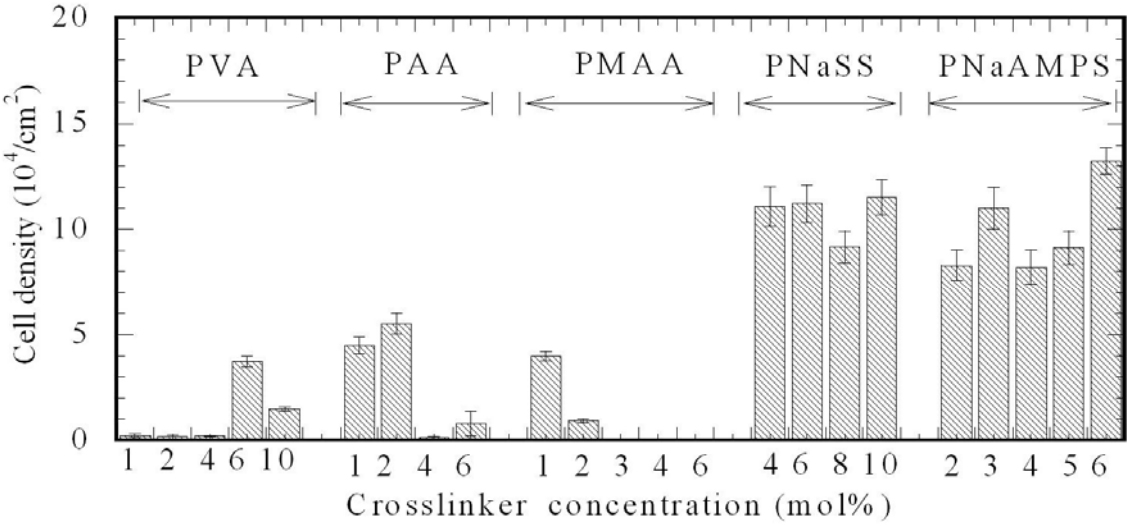
Cell density (10^4/cm^2)
20
15
10
5
0
PVA
PAA
PMAA
PNaSS
PNaAMPS
1 2 4 6 10
1 2 4 6
1 2 3 4 6
4 6 8 10
2 3 4 5 6
Crosslinker concentration (mol%)

Figure 3b

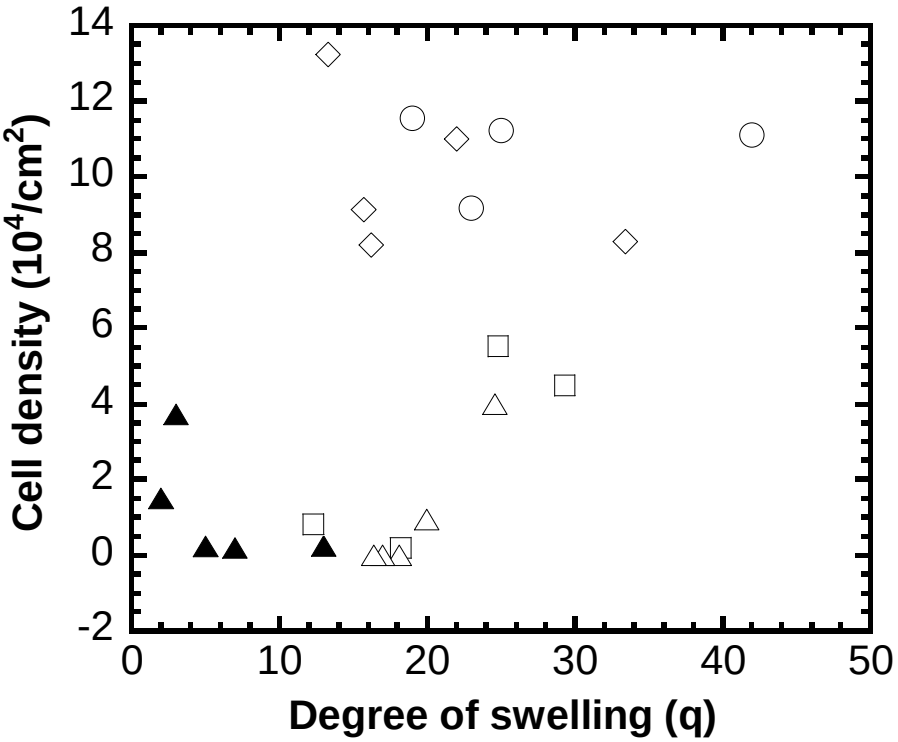
Cell density (10^4/cm^2)
Degree of swelling (q)
14
12
10
8
6
4
2
0
-2
0
10
20
30
40
50

Figure 4a

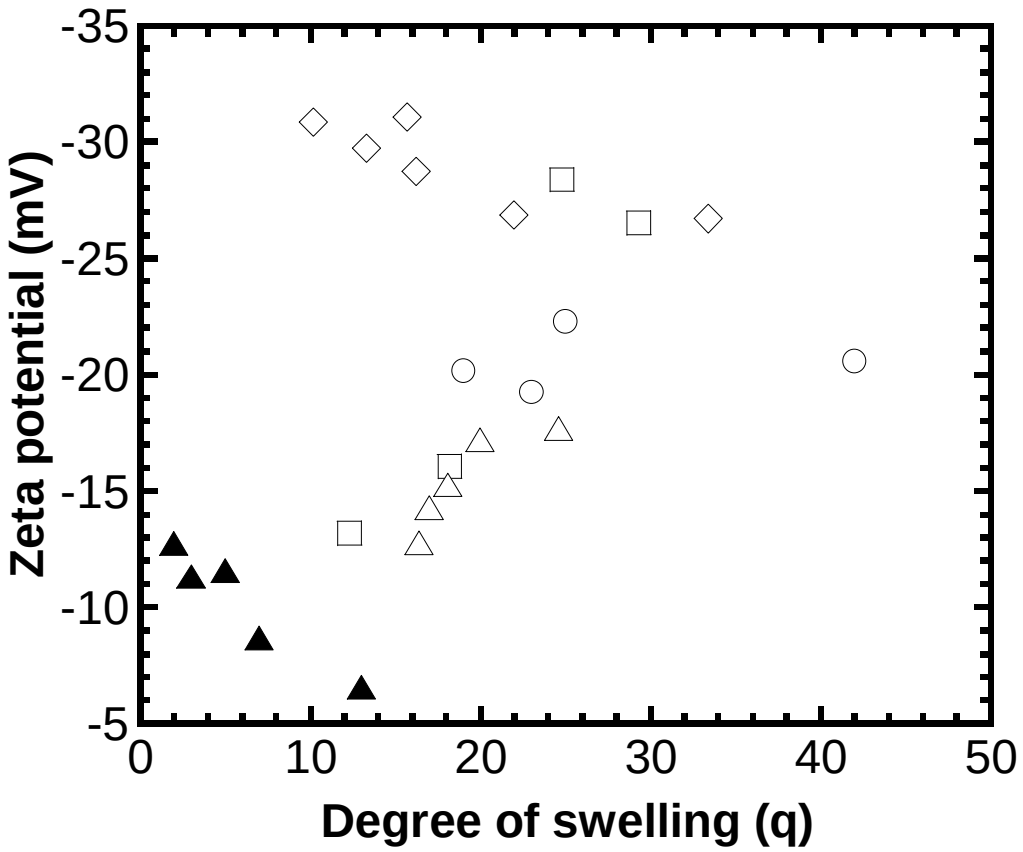
-35
-30
-25
-20
-15
-10
-5
0
10
20
30
40
50
Zeta potential (mV)
Degree of swelling (q)

Figure 4b

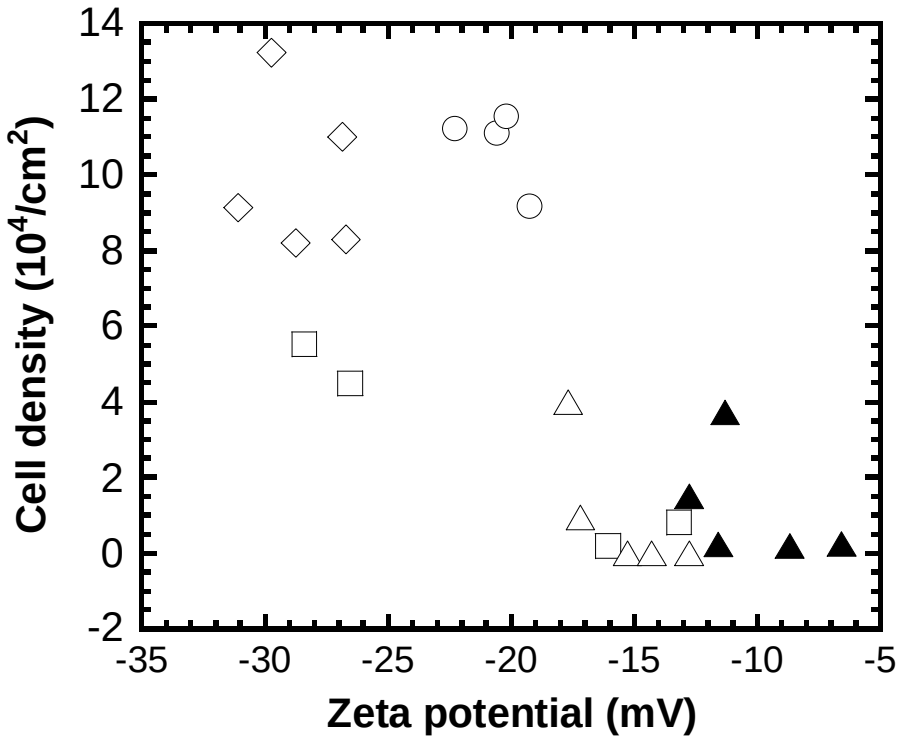
Cell density (10^4/cm^2)
14
12
10
8
6
4
2
0
-2
-35
-30
-25
-20
-15
-10
-5
Zeta potential (mV)

Figure 4c

F	ζ(mV)	BFAECs	HUVECs	RSTFCs
0	-8.8	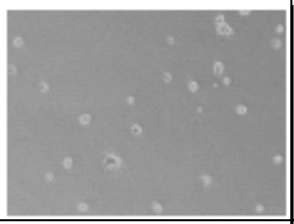	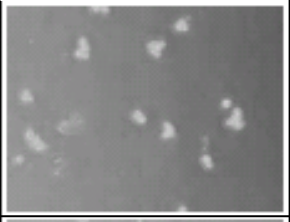	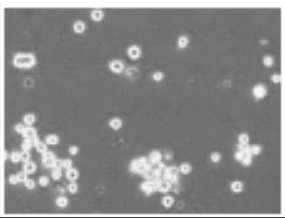
0.3	-10.5	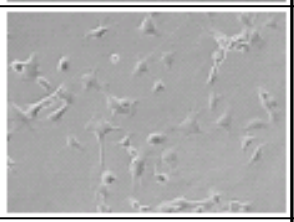	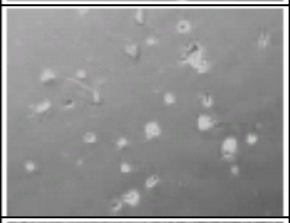	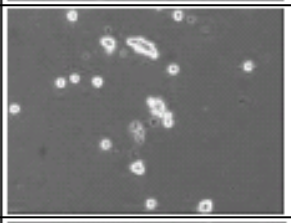
0.4	-16.3	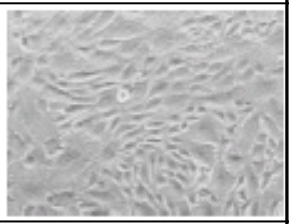	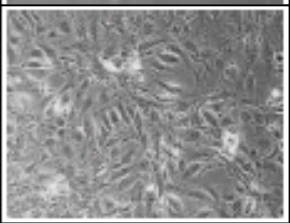	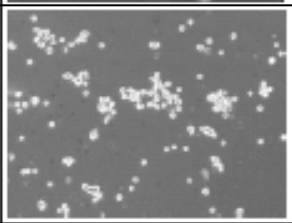
0.5	-20.8	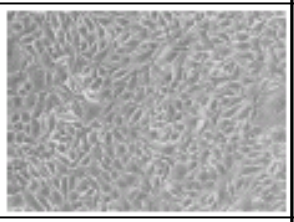	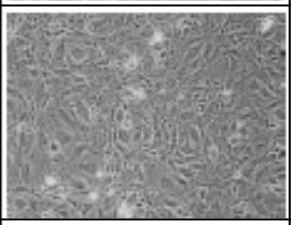	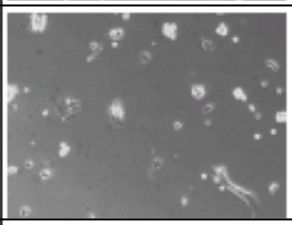
0.7	-22.2	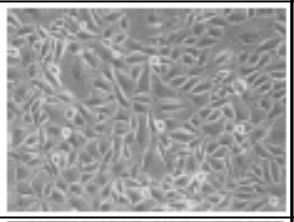	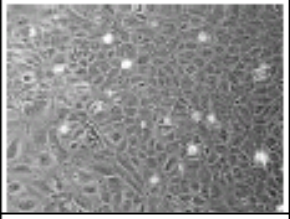	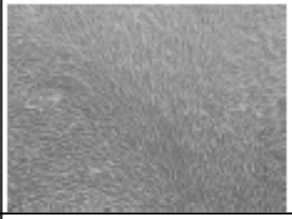
1.0	-28.5	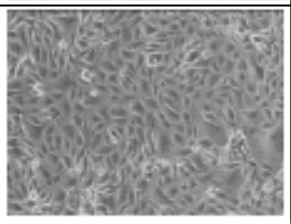	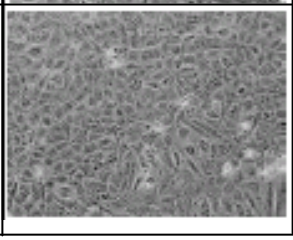	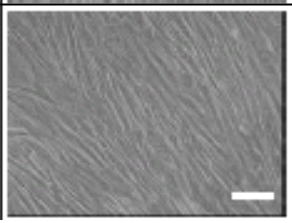

Figure 5

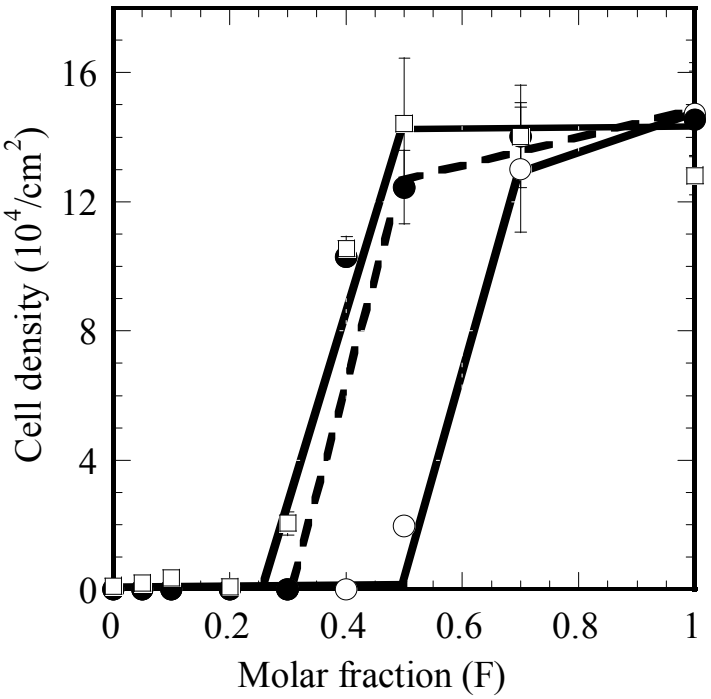

Figure 6

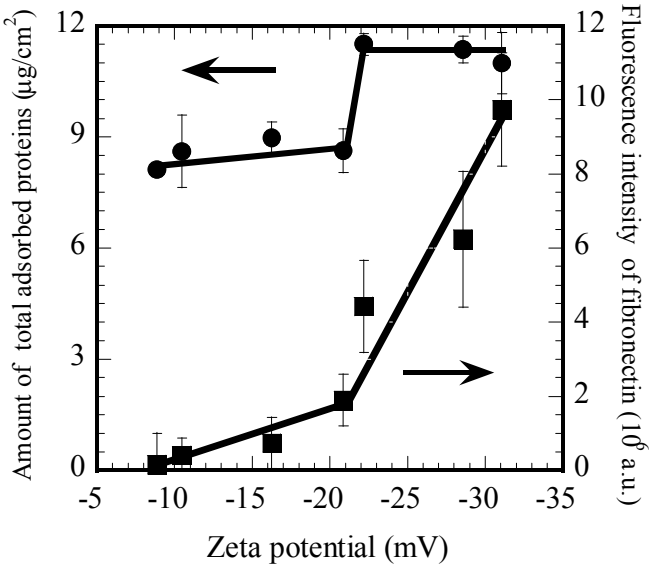
Amount of total adsorbed proteins (μg/cm^2)
Fluorescence intensity of fibronectin (10^6 a.u.)
Zeta potential (mV)
0
3
6
9
12
0
2
4
6
8
10
12
-5
-10
-15
-20
-25
-30
-35

Figure 7

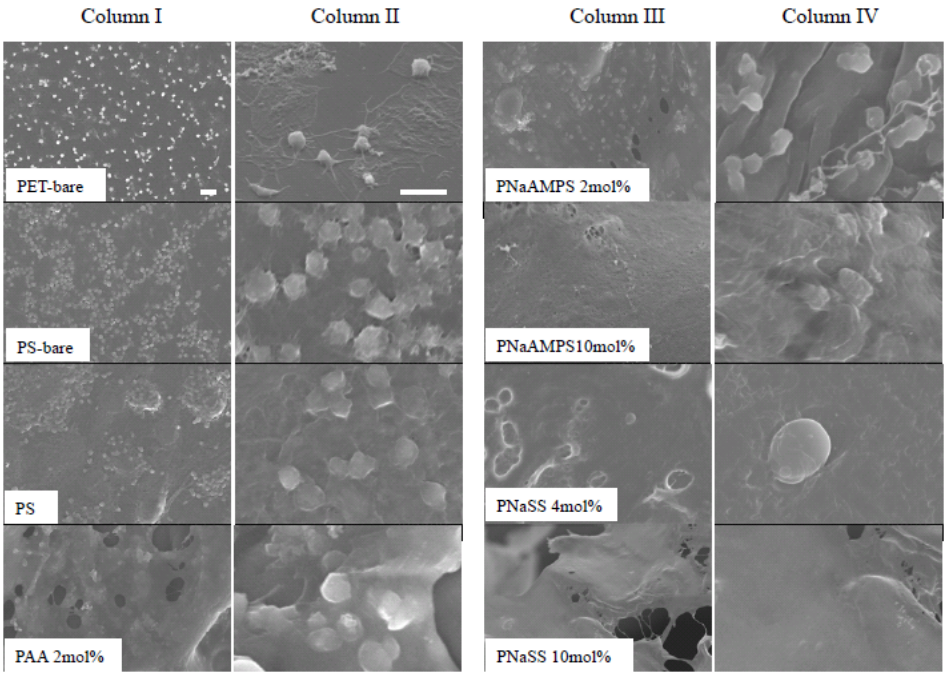
Column I
Column II
Column III
Column IV
PET-bare
PS-bare
PS
PAA 2mol%
PNaAMPS 2mol%
PNaAMPS10mol%
PNaSS 4mol%
PNaSS 10mol%

Figure 8

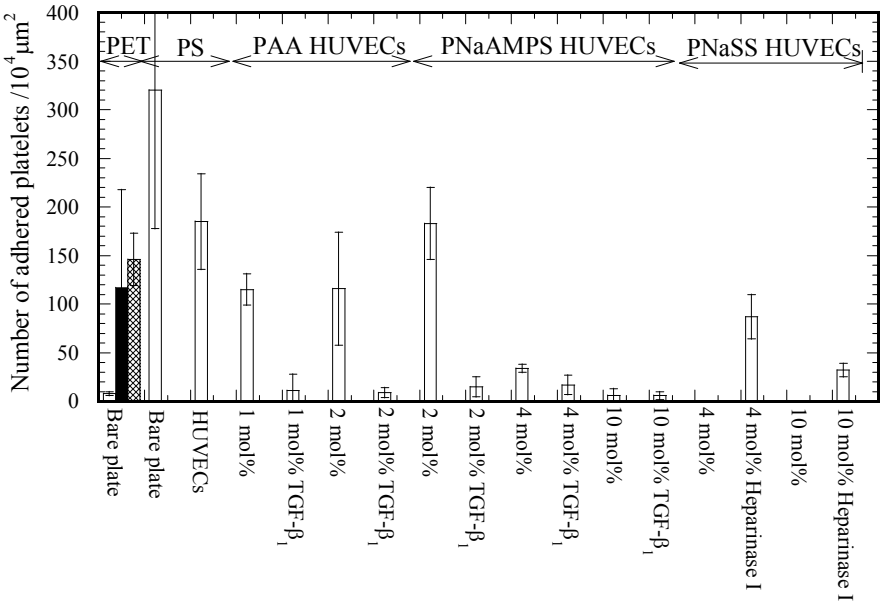
Number of adhered platelets /10^4 µm^2
400
350
300
250
200
150
100
50
0
PET
PS
PAA HUVECs
PNaAMPS HUVECs
PNaSS HUVECs
Bare plate
Bare plate
HUVECs
1 mol%
1 mol% TGF-β$_1$
2 mol%
2 mol% TGF-β$_1$
2 mol%
2 mol% TGF-β$_1$
4 mol%
4 mol% TGF-β$_1$
10 mol%
10 mol% TGF-β$_1$
4 mol%
4 mol% Heparinase I
10 mol%
10 mol% Heparinase I

Figure 9

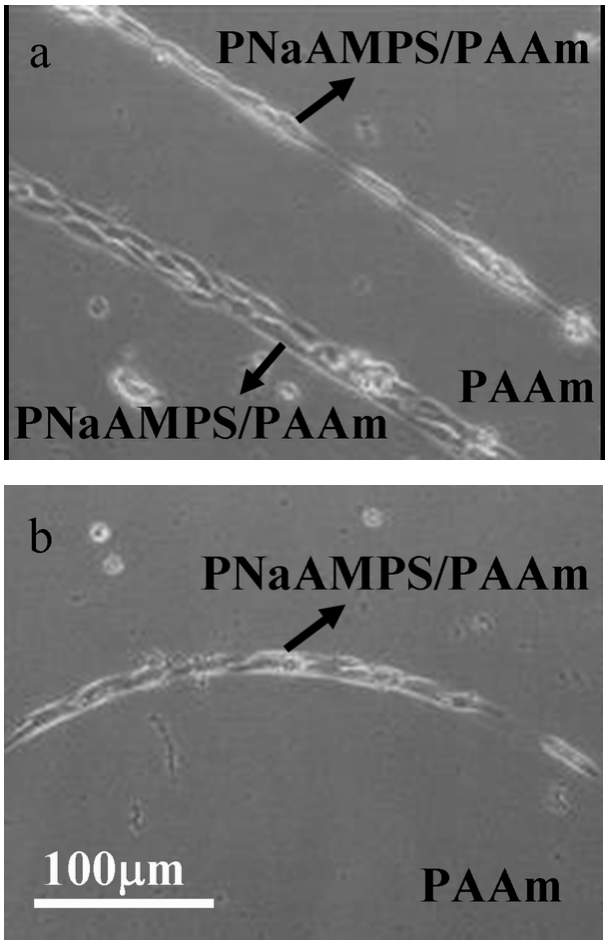

Figure 10

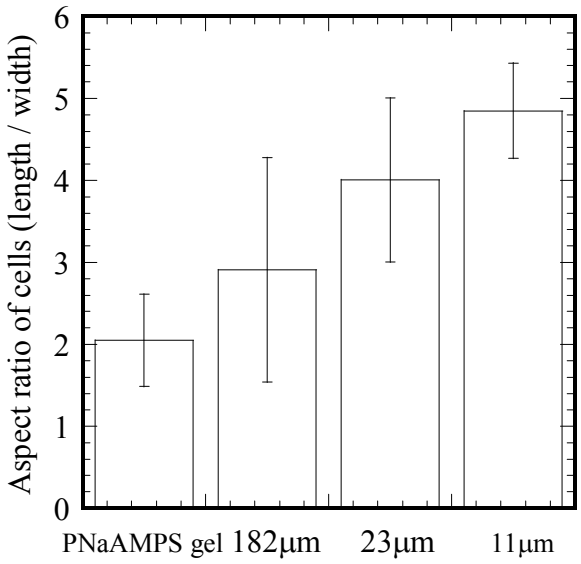
Aspect ratio of cells (length / width)
0
1
2
3
4
5
6
PNaAMPS gel
182μm
23μm
11μm

Figure 11

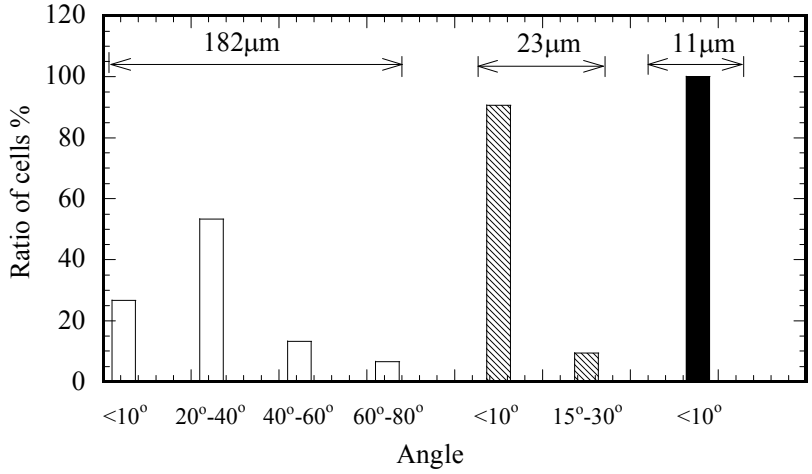
120
100
80
60
40
20
0
Ratio of cells %
182μm
23μm
11μm
<10°
20°-40°
40°-60°
60°-80°
<10°
15°-30°
<10°
Angle

Figure 12

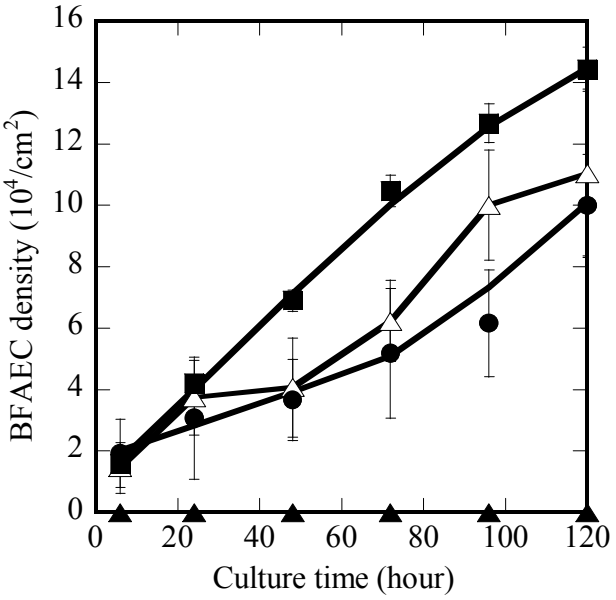
16
14
12
10
8
6
4
2
0
BFAEC density (10^4/cm^2)
0
20
40
60
80
100
120
Culture time (hour)

Figure 13